Journal of Pharmaceutical and Biomedical Analysis 53 (2010) 421–431

Contents lists available at ScienceDirect

Journal of Pharmaceutical and Biomedical Analysis

journal homepage: www.elsevier.com/locate/jpba

Rapid and global detection and characterization of *aconitum* alkaloids in Yin Chen Si Ni Tang, a traditional Chinese medical formula, by ultra performance liquid chromatography–high resolution mass spectrometry and automated data analysis

Guangli Yan[a], Hui Sun[b], Wenjun Sun[b], Li Zhao[b], Xiangcai Meng[b], Xijun Wang[b,*]

[a] *Research Institute of Traditional Chinese Medicine, Heilongjiang University of Chinese Medicine, No. 24 Heping Road, Harbin 150040, PR China*
[b] *Department of Pharmacognosy, Heilongjiang University of Chinese Medicine, No. 24 Heping Road, Harbin, Heilongjiang Province 150040, PR China*

ARTICLE INFO

Article history:
Received 4 March 2010
Received in revised form 29 April 2010
Accepted 1 May 2010
Available online 10 May 2010

Keywords:
Aconitum alkaloids
Yin Chen Si Ni Tang
UPLC/Q-TOF-MS
Metabolynx XS
Mass defect filter

ABSTRACT

An improved method employing Metabolynx XS with mass defect filter (MDF), a post-acquisition data processing software, was developed and applied for global detection of *aconitum* alkaloids in Yin Chen Si Ni Tang, a traditional Chinese medical formula (TCMF). The full-scan LC–MS/MS data sets with extra mass were acquired using ultra performance liquid chromatography coupled with quadrupole-time-of-flight mass spectrometry (UPLC/Q-TOF-MS) with the MS^E mode in a single injection. To remove the interferences, Metabolynx XS was optimized to extract the ions of *aconitum* alkaloids located at the lower abundance. As a result, 62 ions were assigned rapidly to *aconitum* alkaloids and identified tentatively by comparing the accurate mass and fragments information with that of the authentic standards or by mass spectrometry analysis and retrieving the reference literatures. Compared with the previous studies on Fuzi-containing TCMF, the report detected more *aconitum* alkaloids, and the analysis process was accelerated by automated data processing. It is concluded that the screening capability of Metabolynx XS with MDF, together with the utilization of MS^E in structural elucidation, can facilitate a rapid and comprehensive searching and effective structural characterization of *aconitum* alkaloids in TCMF.

1. Introduction

The lateral root of *Aconitum carmichaeli Debx.* (Fuzi) has been used for over 2000 years as an analgesic and cardiotonic herbal medicine in China. Nowadays, *Aconitum* alkaloids have well be known as the main active and toxic components [1–3]. *Aconitum* alkaloids are comprised mainly of C_{19}- and C_{20}-diterpenoid alkaloids. Its structural diversity is derived from the difference between the substituent groups and the substituent positions on the diterpenoid skeleton. Based on the substituents at the C_8 and C_{14} positions of the diterpenoid skeleton, C_{19}-diterpenoid alkaloids can be divided into three major types: diester-diterpenoid alkaloids (DDAs), monoester-diterpenoid alkaloids (MDAs) and alkylolamine-diterpenoid alkaloids (ADAs). C_{20}-diterpenoid alkaloids can be subdivided into three main types: veatchine type, atisine type and delnudine type. The structures of the main known *aconitum* alkaloids in Fuzi are summarized in Table 1 [4].

To date, a number of separation and detection methods have been reported for analyzing the profile of *aconitum* alkaloids and their metabolites, including liquid chromatography/diode array detection (LC/DAD) [5], gas chromatography/mass spectrometry (GC/MS) [6], electrophoresis chromatography/mass spectrometry (EC/MS) [7], and liquid chromatography/mass spectrometry (LC/MS) [4]. However, previous studies only analyzed *aconitum* alkaloids from the single herbal medicine (i.e., Fuzi). A previous study profiled *aconitum* alkaloids in traditional Chinese medical formulas (TCMFs), but only in a limited capacity and only 15 compounds from Fuzi were detected [8]. Fuzi is commonly prescribed as an important ingredient of TCMFs [9], which indicates that analysis of *aconitum* alkaloids in TCMFs is more important. Therefore, developing a rapid and valid method for global detection and characterization of *aconitum* alkaloids in the Fuzi-containing TCMFs is imperative.

Fuzi has to be properly processed to decrease its toxic alkaloids content and make it fit for clinical use [10]. However, processing also results in a large loss of other *aconitum* alkaloids. As a result, *aconitum* alkaloids in Fuzi-containing TCMFs are often present at lower concentration levels; some are present even at trace levels. Moreover, TCMFs consisting of multiple herbal medicines have

* Corresponding author. Tel.: +86 451 82110818; fax: +86 451 82110818.
E-mail address: wxj@hljucm.net (X. Wang).

0731-7085/$ – see front matter.
doi:10.1016/j.jpba.2010.05.004

Table 1
The structures of the main known *aconitum* alkaloids in Fuzi.

Type	Substituent group	Name of compound
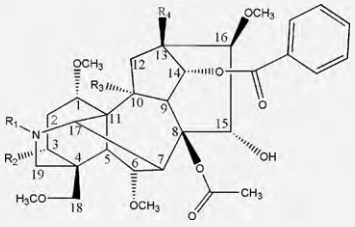	$R_1 = CH_2CH_3$, $R_2 = OH$, $R_3 = H$, $R_4 = OH$ $R_1 = CH_3$, $R_2 = H$, $R_3 = H$, $R_4 = OH$ $R_1 = CH_3$, $R_2 = OH$, $R_3 = H$, $R_4 = OH$ $R_1 = CH_3$, $R_2 = OH$, $R_3 = OH$, $R_4 = OH$ $R_1 = CH_2CH_3$, $R_2 = H$, $R_3 = H$, $R_4 = OH$ $R_1 = CH_2CH_3$, $R_2 = OH$, $R_3 = OH$, $R_4 = OH$ $R_1 = CH_2CH_3$, $R_2 = H$, $R_3 = H$, $R_4 = H$	Aconitine Hypaconitine Mesaconitine Beiwutine Deoxyaconitine Aconifine Penduline
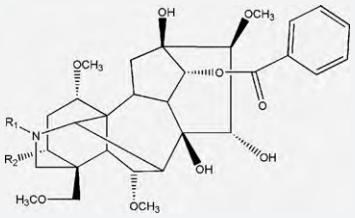	$R_1 = CH_2CH_3$, $R_2 = OH$ $R_1 = CH_3$, $R_2 = H$ $R_1 = CH_3$, $R_2 = OH$	Benzoylaconine Benzoylhypaconine Benzoylmesaconine
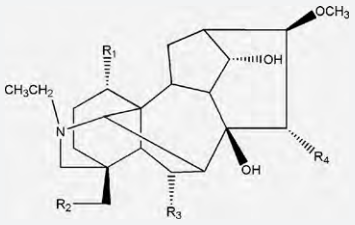	$R_1 = OH$, $R_2 = OCH_3$, $R_3 = OCH_3$, $R_4 = OH$ $R_1 = OH$, $R_2 = OCH_3$, $R_3 = OCH_3$, $R_4 = H$ $R_1 = OH$, $R_2 = OCH_3$, $R_3 = OH$, $R_4 = H$ $R_1 = OCH_3$, $R_2 = OCH_3$, $R_3 = H$, $R_4 = H$ $R_1 = OH$, $R_2 = OCH_3$, $R_3 = H$, $R_4 = OH$ $R_1 = OH$, $R_2 = H$, $R_3 = H$, $R_4 = H$	Fuziline Neoline Senbusine A Talatisamine Senbusine B Karacoline
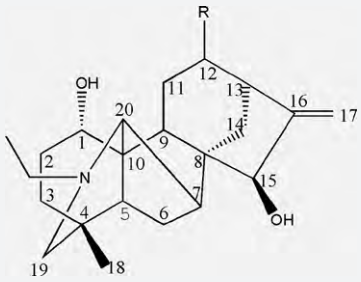	R = Carbonyl R = OH	Songorine Napelline
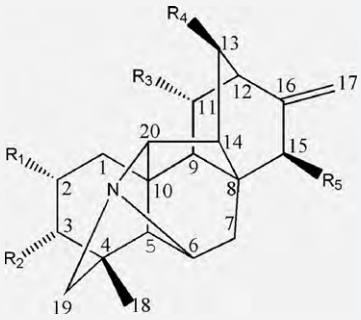	$R_1 = OH$, $R_2 = H$, $R_3 = OH$, $R_4 = OH$, $R_5 = H$ $R_1 = OH$, $R_2 = H$, $R_3 = Ac$, $R_4 = OH$, $R_5 = H$ $R_1 = OH$, $R_2 = OH$, $R_3 = H$, $R_4 = H$, $R_5 = OH$	Hetisine 11-Acetylhetisine 3-Epiignavinol

complicated chemical combinations, making the detection and identification of *aconitum* alkaloids a huge challenge, due to significant interference from other ingredients.

The LC/MS technique has been applied recently to characterize the chemical profiling of TCMF [11]. Ultra performance liquid chromatography–electrospray ionization-quadrupole-time-of-flight mass spectrometry (UPLC–ESI-Q-TOF-MS), in particular, offers rapid and efficient separation and detection methods with accurate mass measurement and tandem mass spectrometry (MS/MS) [12]. However, in most reports using UPLC–ESI-Q-TOF-MS, the inspection of the full-scan mass chromatograms was usually performed manually to screen the components in TCMF. Manual inspection is labour-intensive, and it is difficult to distinguish relatively small signals such as *aconitum* alkaloids from the complex chemical background in full-scan mass chromatograms. Metabolynx XS^{TM}, a spectral and chromatographic searching pro-

gram for post-acquisition data processing, can be used to overcome the problem. Metabolynx XS is capable of automatically processing LC/MS data sets to search expected (targeted) and unexpected (non-targeted) metabolites by comparing the chromatogram of the analyte against the control. The software has been designed specifically to detect and identify metabolites for drug metabolism studies [13]. In addition, a limited application to identify impurities and degradants in pharmaceutical drug products and pesticide metabolites in food samples has also been reported [14,15]. Among the parameters of Metabolynx XS, a mass defect filter (MDF) can conduct selective filtering to remove interferences, such as commonly endogenous chemicals in biological samples, and detect relative drug metabolites utilizing the mass defect difference between drug metabolites and the parent compound [16]. Mass defect refers to the difference between the accurate mass and the nominal mass of an ion. Compared with conventional neutral loss and precursor ion scanning techniques, the MDF technique is more comprehensive in detecting both common (predictable) and uncommon (unpredictable) metabolites [17]. The MDF method has evolved into a comprehensive methodology through a number of successful applications to drug metabolism [18,19]. It is available as a post-acquisition data processing tool for various mass spectrometry vendor software packages, including Metabolynx XS™. In this paper, an improved method employing Metabolynx XS with MDF was developed firstly for rapid detection and characterization of *aconitum* alkaloids under the complicated chemical background of TCMF.

Yin Chen Si Ni Tang (YCSNT) is an TCMF recorded originally in "*Shanghan Weizhi Lun*" during the Song Dynasty [20]. The ingredients of the formula include *Herba Artemisiae Scopariae* (Yinchenhao), Radix Aconiti Lateralis Preparata (prepared Fuzi), Rhizoma Zingiberis (Ganjiang) and Radix et Rhizoma Glycyrrhizae Preparata Cum Melle (prepared Gancao). Traditionally, YCSNT is used for the treatment of liver disorders and jaundice [21]. The four ingredient herbs of YCSNT contain mainly several compound families including flavonoids [22,23], coumarins [22], saponins [23], alkaloids [4], gingerols and shogaols [24]. Among these, flavonoids and coumarins have higher content levels and can generate positive ions in the ESI model, resulting in significant interference with the detection of *aconitum* alkaloids. Therefore, an analysis of *aconitum* alkaloids in YCSNT can illustrate the superiority of the method reported in this paper.

2. Experimental

2.1. Reagents and materials

HPLC grade acetonitrile was purchased from Merck (Darmstadt, Germany). Distilled water was purchased from Watson's Food & Beverage Co., Ltd. (Guangzhou, China). Formic acid was of analytical grade, and was produced from Beijing Reagent Company (Beijing, China). The standard substances of aconitine, mesaconitine, and hypaconitine were purchased from the National Institute for the Control of Pharmaceutical and Biological Products (Beijing, China).

Herba Artemisiae Scopariae was purchased from the China Branch Office of Xinneitian Pharmaceutical Company of Japan (Tianjin, China), *Radix Aconiti Lateralis Preparata* from Zhongba Fuzi Company (Jiangyou, Sichuan, China); *Rhizoma Zingiberis*, and *Rhizoma Glycyrrhizae Preparata Cum Melle* from Harbin Tongrentang Drug Store (Harbin, China). All crude drugs were authenticated by Prof. Xijun Wang, Department of Pharmacognosy of Heilongjiang University of Chinese Medicine. YCSNT was prepared in our laboratory according to the method recorded in "*Shanghan Weizhi Lun*" [20], and the decoction was transformed into the freeze-dried powder.

Table 2
Solvent gradient program of UPLC analysis.

Time (min)	Flow (mL/min)	A (%)	B (%)
0.0	0.5	99.0	1.0
0.5	0.5	90.0	10.0
3.0	0.5	80.0	20.0
8.0	0.5	45.0	55.0
9.0	0.5	1.0	99.0
11.0	0.5	1.0	99.0
11.5	0.5	99.0	1.0
13.0	0.5	99.0	1.0

2.2. Sample preparation

According to the original composition and preparation method of YCSNT recorded in '*Shanghan Weizhi Lun*', the four ingredient herbs including *Herba Artemisiae Scopariae* (6.0 g), *Radix Aconiti Lateralis Preparata* (6.0 g), *Rhizoma Zingiberis* (4.5 g) and *Radix et Rhizoma Glycyrrhizae Preparata Cum Melle* (6.0 g) were mixed and decocted in 400 mL of distilled water for 2 h. The decoction was filtered through 6 layers of gauze, concentrated in vacuum at 60 °C to the level of 0.5 g crude drug per milliliter, and then freeze-dried into the powder.

To prepare the sample of the *Radix Aconiti Lateralis Preparata*-blank YCSNT (RB-YCSNT), *Herba Artemisiae Scopariae* (6.0 g), *Rhizoma Zingiberis* (4.5 g), and *Radix et Rhizoma Glycyrrhizae Preparata Cum Melle* (6.0 g) were mixed and decocted following the same method for preparing YCNST. The resulting decoction was also freeze-dried into powder.

In order to sufficiently illustrate the potential power of the reported method for mining homologous compounds in TCMF using, the sample was subjected to an entire extraction approach to obtain its whole components. 100 mg of the freeze-dried powder of YCSNT was extracted under ultrasonic with 50 mL of methanol for 30 min at room temperature. After shaking, the solution was centrifuged at 13,500 × *g* for 15 min at 4 °C, and the resulting supernatant was used as the sample solution for LC/MS analysis. The sample solutions of RB-YCSNT were prepared using the same treatment method.

2.3. Chromatography and mass spectrometry conditions

LC/MS data were produced using the Waters ACQUITY UPLC® and SYNAPT™ HDMS™ systems (Waters Corporation, Milford, USA) equipped with an electrospray ion source and hybrid quadrupole-time-of-flight (Q-TOF) mass spectrometer with the MS^E model. The system was controlled with Masslynx V4.1. An aliquot of 4 μL of sample solution was injected onto an ACQUITY UPLC BEH C_{18} Column (2.1 mm × 100 mm, 1.7 μm) held at 45 °C. The mobile phase consisted of a linear gradient system of A ($HCOOH:H_2O = 0.1:100$) and B ($HCOOH:CH_3CN = 0.1:100$), and the gradient program is shown in Table 2. The full-scan data were acquired in the positive ion mode from 50 to 1000 Da with a 0.3 s scan time, using a capillary voltage of 2500 V, desolvation temperature of 350 °C, sample cone voltage of 40 V, extraction cone voltage of 4 V, source temperature of 110 °C, cone gas flow of 50 L/h and desolvation gas flow of 500 L/h. The mass spectrometer was calibrated across the mass range of 50–1000 Da using a solution of sodium formate. Data were centroided and mass was corrected during acquisition using an external reference (Lock-Spray™) consisting of a 0.2 ng/mL solution of leucine enkephalin infused at a flow rate of 20 μL min^{-1} via a lockspray interface, generating a reference ion at 556.2771 Da ($[M+H]^+$). The lockspray scan time was set at 0.5 s with the interval of 15 s, and data were averaged over 3 scans.

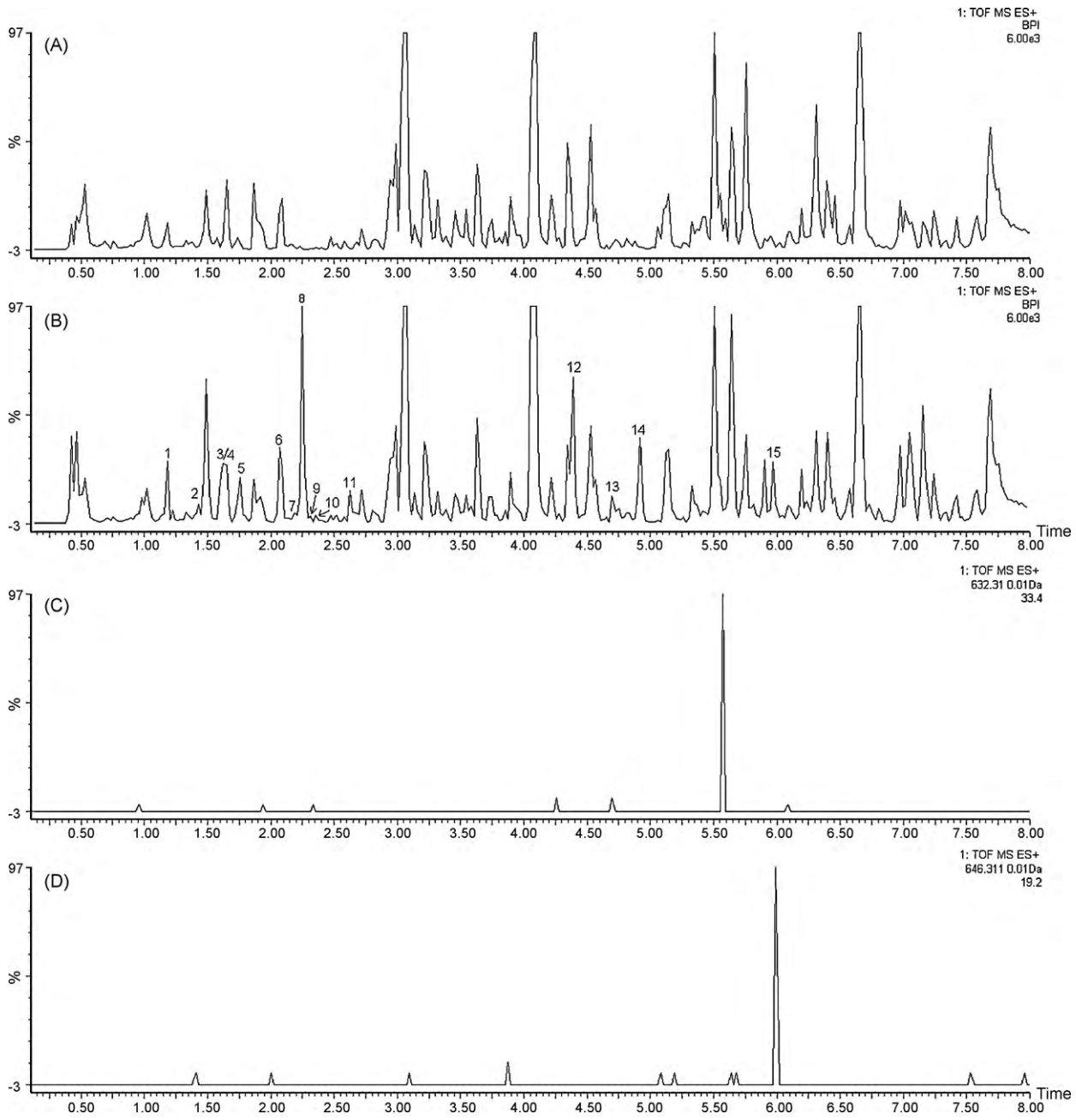

Fig. 1. The low CE chromatograms of RB-YCSNT (A) and YCSNT (B). By extracting the ions at *m*/*z* 646.3102 and *m*/*z* 632.3062 with mass window of 0.01 Da, the extracted ion chromatograms of aconitine (C) and mesaconitine (D) are created.

MS and MS/MS data were acquired using two interleaved scan functions in the MS^E mode. The first scan function was set at 6 V in order to collect information on the intact precursor ions in the sample, and the second scan function was ramped from 10 V to 30 V to obtain the fragment ions data from the ions in the preceding scan.

2.4. Metabolynx XS processing settings

Data files were processed with the Metabolynx XS software package used as a platform to search for expected and unexpected metabolites (compounds) with accurate mass and fragment ions information. The data files from the YCSNT and the RB-YCSNT were specified as 'analyte' and 'control', respectively, to extract the ions from the data sets of the YCSNT which were absent from that of the RB-YCSNT. Songorine ($C_{22}H_{31}NO_3$), Senbusine A ($C_{23}H_{37}NO_6$), and Hypaconitine ($C_{33}H_{45}NO_{10}$) were used as the parent compounds and placed into the columns of Mass A, Mass B and Mass C, respectively. Meanwhile, the three compounds were used as the filtering templates with mass defect range of −38 to +23 mD to carry out the function of MDF. In the window of expected metabolites list, only the parent compound was added, and the mass window was set at 0.01 mD. The unexpected metabolite chromatograms were created over the full acquisition mass range with the mass window of 1 amu. False positives were specified by adding control mass retention times. Peak detection was accomplished with the ApexTrack algorithm, and the threshold of peak area was set at 0.5 unit. The retention time (t_R) filter was applied to extract the chromatograms from 0.5 to 8.0 min. Elemental compositions for unexpected metabolite peaks were generated based on the empirical formula of the parent compound, with no allowance for the change in the number of N atom.

Table 3
Identification and structural characterization of compounds detected in YCSNT by UPLC-Q/TOF-MS with MS^E.

No.	t_R (min)	Measured m/z $[M+H]^+$	Formula $[M+H]^+$	Error (ppm)	Fragment ions (m/z)	Identification
1(1)	1.18	394.2585	$C_{22}H_{36}NO_5$	−2.0	376.2465$[M+H-H_2O]^+$, 358.2351$[M+H-2H_2O]^+$, 340.2292$[M+H-3H_2O]^+$, 328.2289$[M+H-2H_2O-CH_2O]^+$ 322.2106$[M+H-4H_2O]^+$	Chuanfumine
2	1.27	378.2646	$C_{22}H_{36}NO_4$	0.5	360.2504$[M+H-H_2O]^+$, 342.2424$[M+H-2H_2O]^+$	Genicunine A
3	1.37	440.2633	$C_{23}H_{38}NO_7$	−3.4	422.2523$[M+H-H_2O]^+$, 418.2632$[M+H-CH_3OH]^+$, 404.2277$[M+H-2H_2O]^+$	9-Hydroxysenbusine A
4	1.40	424.2675	$C_{23}H_{38}NO_6$	−5.7	406.2617$[M+H-H_2O]^+$, 388.2561$[M+H-2H_2O]^+$, 374.2292$[M+H-H_2O\text{-}CH_3OH]^+$, 356.2242$[M+H-2H_2O-CH_3OH]^+$	Senbusine A
5	1.40	378.2628	$C_{22}H_{36}NO_4$	−4.2	360.2554$[M+H-H_2O]^+$, 342.2454$[M+H-2H_2O]^+$, 332.2183$[M+H-H_2O-C_2H_4]^+$, 324.2365$[M+H-3H_2O]^+$	Carmichaeline
6(2)	1.43	486.2676	$C_{24}H_{40}NO_9$	−5.6	468.2645$[M+H-H_2O]^+$, 454.2513$[M+H-CH_3OH]^+$, 436.2330$[M+H-H_2O-CH_3OH]^+$, 404.2155$[M+H-H_2O-2CH_3OH]^+$	Not identified
7	1.45	364.2479	$C_{21}H_{34}NO_4$	−2.5	346.2374$[M+H-H_2O]^+$, 328.22280$[M+H-2H_2O]^+$	16-β-Hydroxycardiopetaline
8	1.45	394.2597	$C_{22}H_{36}NO_5$	1.0	376.2497$[M+H-H_2O]^+$	Karakolidine
9	1.53	424.2682	$C_{23}H_{38}NO_6$	−4.0	406.2516$[M+H-H_2O]^+$, 388.2487$[M+H-2H_2O]^+$	Senbusine B
10(3)	1.60	378.2639	$C_{22}H_{36}NO_4$	−1.3	360.2514$[M+H-H_2O]^+$, 342.2453$[M+H-2H_2O]^+$, 328.2230$[M+H-H_2O-CH_3OH]^+$, 332.2209$[M+H-H_2O-C_2H_4]^+$, 310.2200$[M+H-2H_2O-CH_3OH]^+$	Karakoline
11(4)	1.62	408.2756	$C_{23}H_{38}NO_5$	1.5	390.2632$[M+H-H_2O]^+$, 372.2538$[M+H-2H_2O]^+$, 358.2371$[M+H-H_2O-CH_3OH]^+$	Isotalatizidine
12	1.67	454.2804	$C_{24}H_{40}NO_7$	−0.1	436.2625$[M+H-H_2O]^+$, 404.2436$[M+H-H_2O-CH_3OH]^+$	Delcosine/Bullatine F/6-Demethyldelsoline
13	1.72	500.2854	$C_{25}H_{42}NO_9$	−1.2	482.2791$[M+H-H_2O]^+$, 468.2633$[M+H-CH_3OH]^+$, 450.2465$[M+H-H_2O-CH_3OH]^+$, 418.2077$[M+H-H_2O-2CH_3OH]^+$	Aconitine
14	1.74	348.2528	$C_{21}H_{34}NO_3$	−3.2	330.2439$[M+H-H_2O]^+$, 312.2357$[M+H-2H_2O]^+$	Dictysine
15(5)	1.76	358.2352	$C_{22}H_{32}NO_3$	−2.2	340.2253$[M+H-H_2O]^+$, 330.2441$[M+H-CO]^+$, 322.2169$[M+H-2H_2O]^+$	Songorine
16	1.58	360.2527	$C_{22}H_{34}NO_3$	−3.3	342.2453$[M+H-H_2O]^+$, 332.2242$[M+H-C_2H_4]^+$, 314.2215$[M+H-H_2O-C_2H_4]^+$	Napalline
17	1.80	330.2056	$C_{20}H_{28}NO_3$	−3.9	312.1906$[M+H-H_2O]^+$, 294.1911$[M+H-2H_2O]^+$	Hetisine
18	1.84	406.2587	$C_{23}H_{36}NO_5$	−1.5	388.2476$[M+H-H_2O]^+$, 370.2361$[M+H-2H_2O]^+$, 360.2278$[M+H-H_2O-C_2H_4]^+$, 328.2111$[M+H-H_2O-C_2H_4-CH_3OH]^+$	Not identified
19	1.94	452.2626	$C_{24}H_{38}NO_7$	−4.9	434.2563$[M+H-H_2O]^+$, 402.2256$[M+H-H_2O-CH_3OH]^+$	Delbruninol
20	2.05	470.2742	$C_{24}H_{40}NO_8$	−2.6	438.22508$[M+H-CH_3OH]^+$	Not identified
21(6)	2.07	454.2802	$C_{24}H_{40}NO_7$	−0.7	436.2682$[M+H-H_2O]^+$, 418.2601$[M+H-2H_2O]^+$, 404.2437$[M+H-H_2O-CH_3OH]^+$, 386.2358$[M+H-2H_2O-CH_3OH]^+$, 372.2178$[M+H-H_2O-2CH_3OH]^+$, 354.2125$[M+H-2H_2O-2CH_3OH]^+$, 322.1870$[M+H-2H_2O-3CH_3OH]^+$	Fuziline
22(7)	2.18	454.2794	$C_{24}H_{40}NO_7$	−2.4	436.2673$[M+H-H_2O]^+$, 404.2460$[M+H-H_2O-CH_3OH]^+$, 372.2241$[M+H-2CH_3OH]^+$	Delcosine/Bullatine F/6-Demethyldelsoline
23(8)	2.25	438.2859	$C_{24}H_{40}NO_6$	−0.7	420.2733$[M+H-H_2O]^+$, 402.2675$[M+H-2H_2O]^+$, 388.2467$[M+H-H_2O-CH_3OH]^+$, 370.2358$[M+H-2H_2O-CH_3OH]^+$, 356.2208$[M+H-H_2O-2CH_3OH]^+$, 338.2185$[M+H-2H_2O-2CH_3OH]^+$, 324.2006$[M+H-H_2O-3CH_3OH]^+$	Neoline
24	2.29	420.2768	$C_{24}H_{38}NO_5$	4.3	402.2607$[M+H-H_2O]^+$, 388.2466$[M+H-CH_3OH]^+$	14-Acetylkarakoline
25	2.31	468.2971	$C_{25}H_{42}NO_7$	2.1		Not identified
26(9)	2.31	450.2844	$C_{25}H_{40}NO_6$	−2.7	432.2752$[M+H-H_2O]^+$, 418.2625$[M+H-CH_3OH]^+$, 386.2328$[M+H-2CH_3OH]^+$	Codelphine
27(10)	2.36	452.2644	$C_{24}H_{38}NO_7$	−0.9	434.2534$[M+H-H_2O]^+$, 402.2229$[M+H-H_2O-CH_3OH]^+$, 374.2212$[M+H-H_2O-CH_3OH-CO]^+$	Dehydrodelcosine
28	2.40	454.2801	$C_{24}H_{40}NO_7$	−0.9	436.2804$[M+H-H_2O]^+$, 422.2453$[M+H-CH_3OH]^+$	Delcosine/Bullatine F/6-Demethyldelsoline
29	2.43	484.2892	$C_{25}H_{42}NO_8$	−3.7	452.2708$[M+H-CH_3OH]^+$, 420.2573$[M+H-2CH_3OH]^+$, 388.2400$[M+H-3CH_3OH]^+$	Pseudaconine

Table 3(*Continued*)

No.	t_R (min)	Measured m/z $[M+H]^+$	Formula $[M+H]^+$	Error (ppm)	Fragment ions (m/z)	Identification
30	2.56	392.2794	$C_{23}H_{38}NO_4$	−1.8	374.2359$[M+H-H_2O]^+$, 360.2525$[M+H-CH_3OH]^+$, 342.2327$[M+H-CH_3OH-H_2O]^+$, 328.2277$[M+H-2CH_3OH]^+$	Sachaconitine
31	2.58	438.2854	$C_{24}H_{40}NO_6$	−0.5	406.2636$[M+H-CH_3OH]^+$, 388.2443$[M+H-CH_3OH-H_2O]^+$, 356.2256$[M+H-2CH_3OH-H_2O]^+$	10-Hydroxytalatizamine
32(11)	2.62	422.2895	$C_{24}H_{40}NO_5$	−2.6	390.2626$[M+H-CH_3OH]^+$, 372.2562$[M+H-CH_3OH-H_2O]^+$, 358.2393$[M+H-2CH_3OH]^+$, 340.2264$[M+H-2CH_3OH-H_2O]^+$	Talatizamine
33	2.64	466.2431	$C_{24}H_{36}NO_8$	−2.1	448.2342$[M+H-H_2O]^+$, 416.2103$[M+H-H_2O-CH_3OH]^+$	Deltamine
34	2.68	344.2582	$C_{22}H_{34}NO_2$	−2.3	326.2587$[M+H-H_2O]^+$	Guanfu base H
35	3.01	420.2387	$C_{23}H_{34}NO_6$	0.0	402.2294$[M+H-H_2O]^+$, 342.1714$[M+H-H_2O-AcOH]^+$	14-Acetylkarakoline
36	3.01	480.2941	$C_{26}H_{42}NO_7$	−4.2	462.2784$[M+H-H_2O]^+$, 430.2694$[M+H-H_2O-CH_3OH]^+$, 398.2441$[M+H-H_2O-2CH_3OH]^+$, 370.1941$[M+H-H_2O-CH_3OH-AcOH]^+$	14-Acetylneoline
37	3.12	452.2988	$C_{25}H_{42}NO_6$	−5.3	420.2724$[M+H-CH_3OH]^+$, 388.2477$[M+H-2CH_3OH]^+$, 356.2207$[M+H-3CH_3OH]^+$	Chasmanine
38	3.25	356.2231	$C_{22}H_{30}NO_3$	1.4	296.2016$[M+H-AcOH]^+$	Not identified
39	3.36	372.2179	$C_{22}H_{30}NO_4$	1.1	354.2201$[M+H-H_2O]^+$, 312.1964$[M+H-AcOH]^+$, 294.1801$[M+H-AcOH-H_2O]^+$	11-Acetylhetisine
40	3.42	434.2898	$C_{25}H_{40}NO_5$	−1.8	402.2540$[M+H-CH_3OH]^+$, 384.2666$[M+H-CH_3OH-H_2O]^+$, 324.2322$[M+H-CH_3OH-H_2O-AcOH]^+$	14-Acetylsachaconitine
41	3.48	464.3018	$C_{26}H_{42}NO_6$	1.3	432.2732$[M+H-CH_3OH]^+$, 414.2684$[M+H-CH_3OH-H_2O]^+$, 400.2493$[M+H-2CH_3OH]^+$, 354.2441$[M+H-CH_3OH-H_2O-AcOH]^+$	14-acetyltalatizamine
42	3.59	606.2925	$C_{31}H_{44}NO_{11}$	1.8	588.2851$[M+H-H_2O]^+$, 574.2659$[M+H-CH_3OH]^+$, 556.2623$[M+H-H_2O-CH_3OH]^+$, 524.2232$[M+H-H_2O-2CH_3OH]^+$, 105.0352$[C_7H_5O]^+$	10-OH Benzoylmesaconine
43	4.06	620.3060	$C_{32}H_{46}NO_{11}$	−1.8	602.2816$[M+H-H_2O]^+$, 588.3002$[M+H-CH_3OH]^+$, 570.2679$[M+H-CH_3OH-H_2O]^+$, 105.0313$[C_7H_5O]^+$	10-OH Benzoylaconine
44	4.34	544.2914	$C_{30}H_{42}NO_8$	0.7	512.2621$[M+H-CH_3OH]^+$,	Not identified
45(12)	4.39	590.2968	$C_{31}H_{44}NO_{10}$	0.5	572.2881$[M+H-H_2O]^+$, 558.2700$[M+H-CH_3OH]^+$, 540.2556$[M+H-H_2O-CH_3OH]^+$, 526.2409$[M+H-2CH_3OH]^+$, 508.2338$[M+H-H_2O-2CH_3OH]^+$, 105.0349$[C_7H_5O]^+$	Benzoylmesaconine
46	4.59	540.2938	$C_{31}H_{42}NO_7$	−4.3	522.2828$[M+H-H_2O]^+$, 504.2788$[M+H-2H_2O]^+$, 462.2704$[M+H-2H_2O-CH_3OH]^+$, 444.2449$[M+H-3H_2O-CH_3OH]^+$, 340.2131$[M+H-2H_2O-CH_3OH-BzOH]^+$, 322.2170$[M+H-3H_2O-CH_3OH-BzOH]^+$, 105.0347$[C_7H_5O]^+$	Not identified
47(13)	4.70	604.3122	$C_{32}H_{46}NO_{10}$	0.0	586.2988$[M+H-H_2O]^+$, 572.2855$[M+H-CH_3OH]^+$, 554.2726$[M+H-H_2O-CH_3OH]^+$, 540.2526$[M+H-2CH_3OH]^+$, 522.2428$[M+H-2CH_3OH-H_2O]^+$, 490.2107$[M+H-3CH_3OH-H_2O]^+$, 105.0347$[C_7H_5O]^+$	Benzoylaconine
48	4.73	558.3063	$C_{31}H_{44}NO_8$	−0.7	526.2833$[M+H-CH_3OH]^+$, 508.2677$[M+H-CH_3OH-H_2O]^+$, 476.2491$[M+H-2CH_3OH-H_2O]^+$, 105.0354$[C_7H_5O]^+$	Benzoyl-3,13-deoxyaconine
49(14)	4.92	574.3019	$C_{31}H_{44}NO_9$	0.5	542.2721$[M+H-CH_3OH]^+$, 524.2566$[M+H-CH_3OH-H_2O]^+$, 510.2503$[M+H-2CH_3OH]^+$, 492.2406$[M+H-2CH_3OH-H_2O]^+$, 460.2160$[M+H-3CH_3OH-H_2O]^+$, 388.2058$[M+H-2CH_3OH-BzOH]^+$, 105.0357$[C_7H_5O]^+$	Benzoylhypaconine
50	5.08	572.2849	$C_{31}H_{42}NO_9$	−1.9	554.2780$[M+H-H_2O]^+$, 540.2563$[M+H-CH_3OH]^+$, 522.2511$[M+H-CH_3OH-H_2O]^+$, 490.2105$[M+H-2CH_3OH-H_2O]^+$, 105.0370$[C_7H_5O]^+$	Pyromesaconitine/16-Epipyromesaconitine
51	5.17	558.3066	$C_{31}H_{44}NO_8$	−0.2	540.2875$[M+H-H_2O]^+$, 526.2775$[M+H-CH_3OH]^+$, 508.2671$[M+H-H_2O-CH_3OH]^+$, 494.2805$[M+H-2CH_3OH]^+$, 105.0347$[C_7H_5O]^+$	Benzoyl-3,13-deoxyaconine
52	5.19	648.3005	$C_{33}H_{46}NO_{12}$	−2.3	630.2770$[M+H-H_2O]^+$, 616.2545$[M+H-CH_3OH]^+$, 105.0369$[C_7H_5O]^+$, 598.2775$[M+H-H_2O-CH_3OH]^+$, 588.3013$[M+H-AcOH]^+$, 570.2441$[M+H-AcOH-H_2O]^+$, 556.2762$[M+H-AcOH-CH_3OH]^+$,	Beiwutine

53	5.21	588.3160	$C_{32}H_{46}NO_9$	−2.2	556.2900[M+H−CH_3OH]$^+$, 524.2725[M+H−2CH_3OH]$^+$, 492.2373[M+H−3CH_3OH]$^+$, 105.0370[C_7H_5O]$^+$		Benzoyldeoxyaconine
54	5.51	542.3126	$C_{31}H_{44}NO_7$	1.5	510.2854[M+H−CH_3OH]$^+$, 492.2787[M+H−CH_3OH−H_2O]$^+$, 460.2506[M+H−2CH_3OH−H_2O]$^+$, 105.0355[C_7H_5O]$^+$		Benzoylneoline
55	5.57	632.3062	$C_{33}H_{46}NO_{11}$	−1.4	600.2848[M+H−CH_3OH]$^+$, 582.2836[M+H−CH_3OH−H_2O]$^+$, 572.2880[M+H−AcOH]$^+$, 540.2609[M+H−AcOH−CH_3OH]$^+$, 522.2512[M+H−AcOH−CH_3OH−H_2O]$^+$, 105.0355[C_7H_5O]$^+$		Mesaconitine
56	5.59	558.3058	$C_{31}H_{44}NO_8$	−1.6	540.273[M+H−H_2O]$^+$, 522.2587[M+H−2H_2O]$^+$, 490.2279[M+H−2H_2O−CH_3OH]$^+$, 105.0382[C_7H_5O]$^+$		Benzoyl-3,13-deoxyaconine
57	5.62	662.3177	$C_{34}H_{48}NO_{12}$	0.0	602.2964[M+H−AcOH]$^+$, 570.2786[M+H−AcOH−CH_3OH]$^+$, 552.2709[M+H−AcOH−CH_3OH−H_2O]$^+$, 105.0360[C_7H_5O]$^+$		Aconifine
58	5.88	572.3214	$C_{32}H_{46}NO_8$	−1.6	540.2979[M+H−CH_3OH]$^+$, 508.2683[M+H−2CH_3OH]$^+$, 105.0364[C_7H_5O]$^+$		Pyromesaconitine/16-Epipyromesaconitine
59(15)	5.97	616.3135	$C_{33}H_{46}NO_{10}$	2.1	584.2803[M+H−CH_3OH]$^+$, 556.2857[M+H−AcOH]$^+$, 524.2657[M+H−AcOH−CH_3OH]$^+$, 496.2714[M+H−AcOH−CH_3OH−CO]$^+$, 492.2338[M+H−AcOH−2CH_3OH]$^+$, 338.1749[M+H−AcOH−3CH_3OH−BzOH]$^+$, 105.0337[C_7H_5O]$^+$		Hypaconitine
60	5.99	646.3102	$C_{34}H_{48}NO_{11}$	3.6	586.3029[M+H−AcOH]$^+$, 554.2768[M+H−AcOH−CH_3OH]$^+$, 464.2409[M+H−AcOH−BzOH]$^+$, 105.0352[C_7H_5O]$^+$		Aconitine
61	6.04	600.3187	$C_{33}H_{46}NO_9$	2.3	540.2874[M+H−AcOH]$^+$, 508.2682[M+H−AcOH−CH_3OH]$^+$, 580.2682[M+H−AcOH−CH_3OH−CO]$^+$, 448.2482[M+H−AcOH−2CH_3OH−CO]$^+$, 105.0373[C_7H_5O]$^+$		Delphinine
62	6.38	630.3273	$C_{34}H_{48}NO_{10}$	−0.8	598.33061[M+H−CH_3OH]$^+$, 570.3039[M+H−AcOH]$^+$, 538.2808[M+H−AcOH−CH_3OH]$^+$, 510.2765[M+H−AcOH−CH_3OH−CO]$^+$, 478.2595[M+H−AcOH−2CH_3OH−CO]$^+$, 105.0348[C_7H_5O]$^+$		Deoxyaconitine

Number in parenthesis represents the no. of peaks labeled in Fig. 1(B).

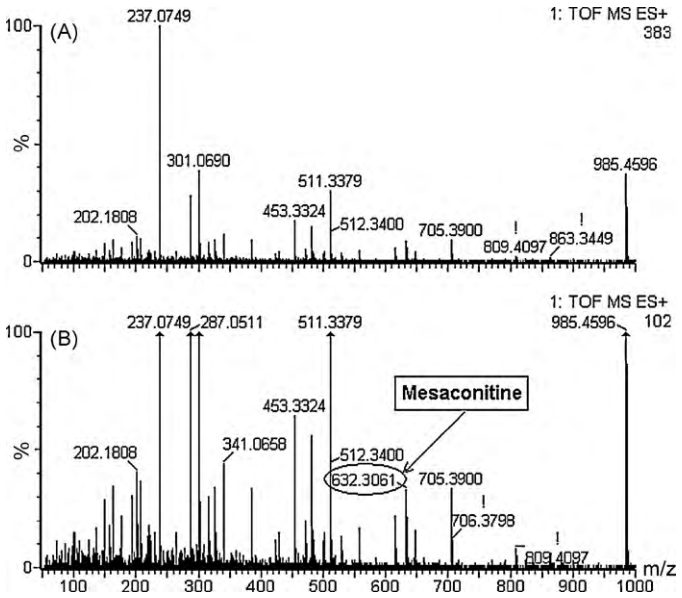

Fig. 2. The mass spectra before (A) and after (B) zoomed in at the retention time of 5.57 min. The precursor ion of mesaconitine in the mass spectrum zoomed in is highlighted with the elliptical cycle.

3. Results and discussion

3.1. Peaks detection

Utilizing the MS^E technique, two distinct mass chromatograms were produced in the positive ion model from both the low and high CE data channels in a single LC injection. One at the low CE contained protonated molecular ion ([M+H]$^+$) information, which was used to analyze the profile of the constituents in YCSNT. The other at high CE contained fragment ions information for structural characterization of the corresponding ion. Fig. 1(A) and (B) shows the BPI chromatograms at the low CE of RB-YCSNT and YCSNT, respectively. The constituents in YCSNT were well separated using the UPLC–ESI-Q-TOF-MS system with high sensitivity and high resolution; 15 peaks were labeled as *aconitum* alkaloids through manual inspection and elucidation of the data at the high and low CE of the peaks. The proper identifications are provided in Table 3. However, some *aconitum* alkaloids ions with the lower abundance were embedded in the background ions, resulting in the compounds being missed easily during the manual inspection. For example, two ions of *m*/*z* 632.3106 at 5.57 min and *m*/*z* 646.3114 at 5.99 min, which were identified as mesaconitine and aconitine, respectively, through a comparison of the retention time, accurate mass, and fragment ions with those of the authentic standards, could not be labeled in Fig. 1(B). Moreover, the interference of other ions caused difficulties in locating the two ions from the respective mass spectrum and resulted in their omission. Creating the extracted ion chromatograms (Fig. 1(C) and (D)) or zooming in the mass spectra (Figs. 2 and 3) allowed the ions to be detected. However, the searching method was invalid for the unknown *aconitum* alkaloids. Therefore, it was difficult to perform global detection of *aconitum* alkaloids in YCSNT through manual inspection.

MetaboLynx XS is a post-acquisition data processing software that can be applied to the full-scan data files in dividually or in batch format. By comparing the data files of the analyte (commonly sample containing metabolites, here the YCSNT sample) against the control (usually a blank sample, here the RB-YCSNT sample), this software automates the detection, identification, and reporting of expected and unexpected ions peaks in a faster and more complete manner than a manual inspection according to the processing set-

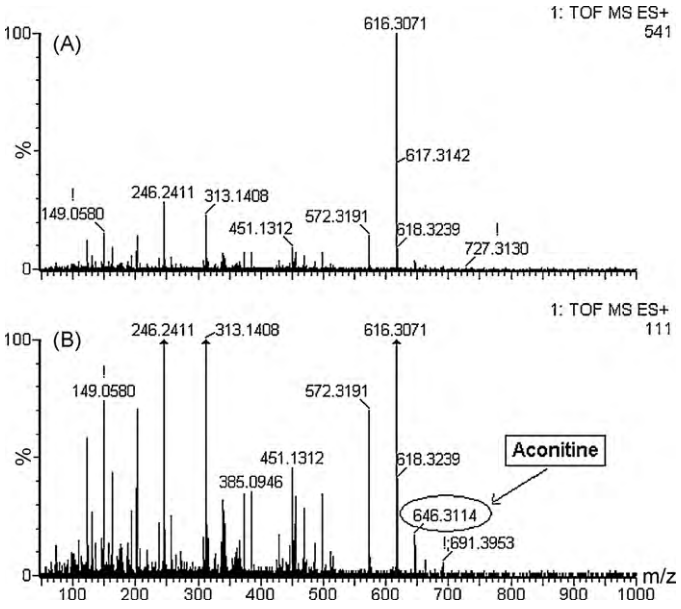

Fig. 3. The mass spectra before (A) and after (B) at the retention time of 5.99 min. The precursor ion of aconitine in the mass spectrum zoomed in is highlighted with the elliptical cycle.

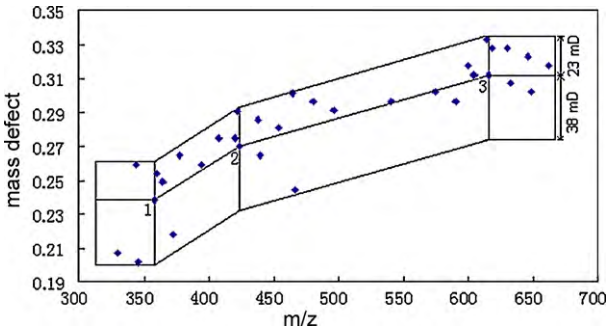

Fig. 4. Mass defect profile of the known *aconitum* alkaloids in Fuzi. Pots 1, 2 and 3 represent Songorine (357.2304), Senbusine A (423.2621) and Hypaconitine (615.3043), respectively.

tings. The extracted ions were listed as expected and unexpected. An expected metabolite is a compound intentionally searched for in the data files based on the specific mass difference from the parent compound (the template), while an unexpected one is not intentionally searched for but whose existence is proposed based on a comparison between the analyte and the control. In other words, the former is targeted and the later untargeted. Therefore, MetaboLynx XS can be used to perform a global detection through the two searching channels based on the correct parameter settings.

The processing settings are the keys to finding both expected (targeted) and unexpected (untargeted) metabolites (compounds). Of all the settings, the filter template and the mass defect range are considered to be the most intellective parameters because the settings can remove interference compounds without filtering true metabolites. Zhang et al. illustrated the effect of MDF on the chromatograms of the biological samples, and a broad applicability of MDF for selective detection of drug metabolites was suggested [18].

Table 4
Formulas and the relative mass information of the known *aconitum* alkaloids in Fuzi.

No.	Compound	Formula	Molecular weight	Mass defect
1	Aconitine	$C_{34}H_{47}NO_{11}$	645.3023	0.3023
2	Hypaconitine	$C_{33}H_{45}NO_{10}$	615.3043	0.3043
3	Mesaconitine	$C_{33}H_{45}NO_{11}$	631.2993	0.2993
4	8-OEt-14-benzoylmesaconine	$C_{33}H_{47}NO_{10}$	617.3200	0.3200
5	Beiwutine	$C_{33}H_{45}NO_{12}$	647.2942	0.2942
6	Aconifine	$C_{33}H_{47}NO_{11}$	661.2921	0.2921
7	Deoxyaconitine	$C_{34}H_{47}NO_{10}$	629.3200	0.3200
8	Penduline	$C_{34}H_{47}NO_{9}$	613.3251	0.3251
9	Chasmaconitine	$C_{34}H_{47}NO_{9}$	613.3251	0.3251
10	Delphinine	$C_{33}H_{45}NO_{9}$	599.3094	0.3094
11	Benzoylhypaconine	$C_{31}H_{43}NO_{9}$	573.2938	0.2938
12	Benzoylaconine	$C_{32}H_{45}NO_{10}$	603.3043	0.3043
13	Benzoylmesaconine	$C_{31}H_{43}NO_{10}$	589.2887	0.2887
14	16-β-Hydroxycardiopetaline	$C_{21}H_{33}NO_{4}$	363.2410	0.2410
15	9-Hydroxysenbusine A	$C_{23}H_{37}NO_{7}$	439.2570	0.2570
16	14-Benzoylneoline	$C_{31}H_{43}NO_{7}$	541.3040	0.3040
17	Fuziline	$C_{24}H_{39}NO_{7}$	453.2727	0.2727
18	Neoline	$C_{24}H_{390}NO_{6}$	437.2777	0.2777
19	Talatizamine	$C_{24}H_{39}NO_{5}$	421.2828	0.2828
20	14-Acetyltalatizamine	$C_{26}H_{41}NO_{6}$	463.2948	0.2948
21	Isotalatizidine	$C_{23}H_{37}NO_{5}$	407.2672	0.2672
22	Talatizamine	$C_{24}H_{39}NO_{5}$	421.2828	0.2828
23	10-Hydroxytalatizamine	$C_{24}H_{39}NO_{6}$	437.2777	0.2777
24	14-Acetylneoline	$C_{26}H_{41}NO_{7}$	479.2883	0.2883
25	8-Acetyl-15-hydroxyneoline	$C_{26}H_{41}NO_{8}$	495.2832	0.2832
26	Senbusine A	$C_{23}H_{37}NO_{6}$	423.2621	0.2621
27	Karakoline	$C_{22}H_{35}NO_{4}$	377.2566	0.2566
28	14-Acetylkarakoline	$C_{24}H_{37}NO_{5}$	419.2672	0.2672
29	Karakolidine	$C_{22}H_{35}NO_{5}$	393.2515	0.2515
30	Songorine	$C_{22}H_{31}NO_{3}$	357.2304	0.2304
31	Napelline	$C_{22}H_{33}NO_{3}$	359.2460	0.2460
32	Chuanfumine	$C_{22}H_{35}NO_{5}$	393.2515	0.2515
33	Hetisine	$C_{20}H_{27}NO_{3}$	329.1991	0.1991
34	Guanfu base H	$C_{22}H_{33}NO_{2}$	343.2504	0.2504
35	11-Acetylhetisine	$C_{22}H_{29}NO_{4}$	371.2097	0.2097
36	3-Epiignavinol	$C_{20}H_{27}NO_{4}$	345.1940	0.1940
37	Unknown	$C_{24}H_{35}NO_{8}$	465.2363	0.2363
38	Unknown	$C_{31}H_{41}NO_{7}$	539.2833	0.2833

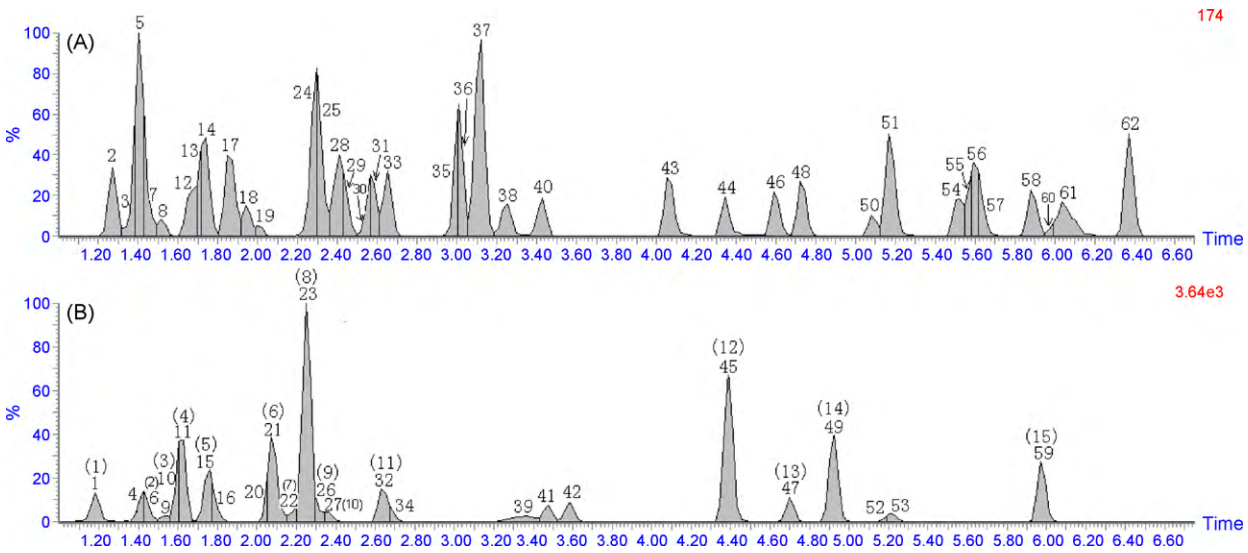

Fig. 5. The extracted ions chromatograms of *aconitum* alkaloids in YCSNT displayed in Metabolynx. For clear labeling, the extracted ions chromatograms are combined into two fingerprints based on the peak intensity. Peak numbers are consistent with those in Table 3.

However, the application of this type of filtering has to be performed carefully since some ions may be missed when it is used incorrectly. Hence, the selection of the filtering templates and the calculation of the mass defect difference of potential metabolites (or interesting compounds) relative to the templates play a key role in the global detection of potential metabolites. Zhu et al. demonstrated the use of structure-based filter templates for calculating appropriate settings for MDF [17]. In this paper, a mass defect-based method was suggested to select appropriate templates and calculate the window of MDF. Table 4 lists the relative mass information of the known *aconitum* alkaloids in Fuzi according to the literature [4], and the mass defect profile of the listed compounds is shown in Fig. 4 wherein each dot represents the accurate mass of a compound. Choosing just a single parent compound, the mass defect range covering all *aconitum* alkaloids would be considerably wide such that a large number of interference compounds would be involved. However, if multiple parent compounds were used, a template curve connecting these compounds could be produced to implement a dynamically ramped filtering, and the curve automatically extended by 50 Da to both sides in the direction of m/z. Here, three compounds, namely Songorine, Senbusine A and Hypaconitine, were selected as parent compounds to form a filtering curve, and the window of −38 to +23 mD was set to minimize the mass defect range. Hence, a region with the filtering curve as the central axis and the filtering window as the limit covering all *aconitum* alkaloids listed in Table 4 was produced (Fig. 4). All compounds whose molecular weights are situated within the region can be detected and the unknown *aconitum* alkaloids can also be discovered.

Due to the lower concentration levels of some *aconitum* alkaloids such as mesaconitine and aconitine, the absolute peak area threshold in the parameters setting was lowered significantly to 0.5 unit to ensure the highest possible detection of these peaks; however, lowering the threshold also resulted in the addition of a few background noise peaks. To minimize this effect, visual inspection was necessary for conducting an accurate assessment of the extracted ions.

After being optimized, Metabolynx XS was used to process the full-scan chromatogram of YCSNT. A total of 145 ions with information on m/z, area, t_R, formula, etc. were extracted from the full-scan chromatogram and displayed in the lists of expected and unexpected compounds. Among the compounds, 56 ions were labeled as false positives and were immediately excluded; 27 ions were also eliminated rapidly by manual inspection based on the molecular formulas and the fragments characterizations. These will be described in detail in the next section. As a result, 62 ions were assigned rapidly to *aconitum* alkaloids (listed in Table 3). For clear labeling, the extracted ion chromatograms combined in Metabolynx XS are shown with two fingerprints (Fig. 5). The fingerprints indicate that Metabolynx XS can perform global analysis of *aconitum* alkaloids in YCSNT in comparison with manual inspection.

Among the compounds detected, some were present at extremely low concentration levels; however, considering that some *aconitum* alkaloids such as aconitine and mesaconitine are highly bioactive and toxic, it is essential that a detection of the compounds be performed. Compared with the previous studies on Fuzi-containing TCMF [8], the report detected more *aconitum* alkaloids, and the analysis process was accelerated with automated data processing.

3.2. Structural characterization of aconitum alkaloids

The fragmentation pathways of *aconitum* alkaloids have been investigated and summarized previously [4]. The compounds share the common principal fission pattern of successive or simultaneous losses of 1–3 H_2O or 1–4 CH_3OH in peripheral moieties. In addition, for DDAs, the characteristic losses of AcOH and BzOH can be observed, and the benzoyl cation $[C_7H_5O]^+$ indicating the presence of a benzoyl group can be detected. The neutral loss of 28 Da can be explained by the loss of CO (27.9949) or C_2H_4 (28.0313) based on accurate elemental compositions of product ions. For ADAs the neutral loss of C_2H_4 from the N atom can usually be observed. The rule of elimination of substituents in ESI-MS were also analyzed. The methoxy at the C_{16} position was initially missed, and then C_1, C_6, and C_{18} [25]. For the hydroxyl, C_1 was the most active site for ADAs, and its loss was observed as the base peak to deduce the presence of hydroxyl at the C_1 position [4].

In this report, the high-resolution Q-TOF/MS was used to provide accurate mass measurement, from which the elemental compositions of the ions were deduced. The scan function at the high CE was used to collect exact mass fragment ions data in an unbiased manner equivalent to a non-selective tandem mass spectrometric scan. Plumb has demonstrated a method of elucidating the mass spectra from complex mixtures acquired with MS^E [26]. However, for the complex mixtures of TCMF, a comparison of the difference ions between the high and low CE mass spectra and the exact mass difference between the ions in the high CE mass

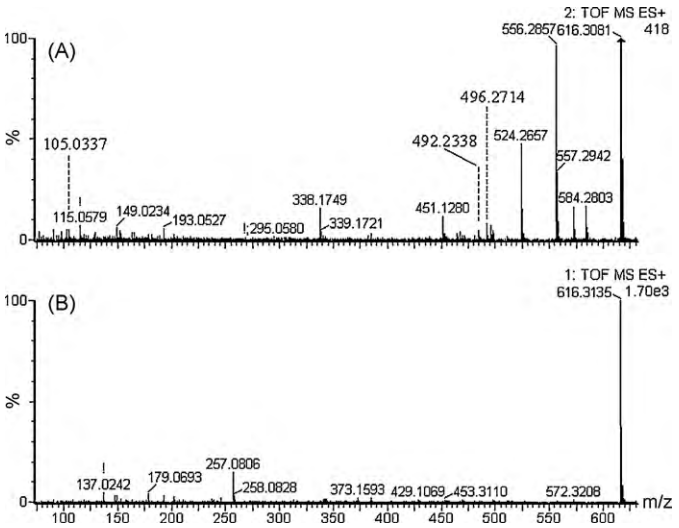

Fig. 6. The high (A) and low (B) CE mass spectra at the retention time of 5.97 min.

spectrum and the corresponding precursor ion is not sufficient. This is because these numerous ions in the high CE mass spectrum interfere significantly with the assignment of fragment ions. If fragment characterizations of the precursor ion have also been applied together with the method demonstrated in the literature, the fragment ions can be searched for rapidly and in a targeted manner.

Fig. 6 shows the high and low CE mass spectra of the peak at retention time of 5.97 min. The mass spectrum at the low CE displays the protonated molecular ions among which the ion at *m*/*z* 616.3135 had a highest abundance. The corresponding fragment ions are shown in the high CE spectrum. Based on the elucidation method described above, the ions at *m*/*z* 584.2803 ($[M+H-CH_3OH]^+$), 556.2857 ($[M+H-AcOH]^+$), 524.2657 ($[M+H-AcOH-CH_3OH]^+$), 496.2714 ($[M+H-AcOH-CH_3OH-CO]^+$), 492.2338 ($[M+H-AcOH-2CH_3OH]^+$), 338.1749 ($[M+H-AcOH-3CH_3OH-BzOH]^+$), and 105.0337 ($[C_7H_5O]^+$) were assigned rapidly as product ions of the precursor ion at *m*/*z* 616.3135 ($[M+H]^+$). If the fragmentation characterization of Hypaconitine had not been applied, the fragment ions at *m*/*z* 496.2714, 492.2338 and 105.0337 would have been omitted. By comparing the accurate molecular mass and fragmenting characterizations with those of the authentic standard, the compound was identified as Hypaconitine. The example also illustrated that the fragment ions generated by MS^E in a single analytical run was similar to those followed by conventional MS^n [4]. Based on the elucidation method, the detected ions were tentatively identified and shown in Table 3. Some peaks had the same *m*/*z* value of quasimolecular ion and similar fragment ions, including peaks 13, 22, and 28; peaks 50 and 58; and peaks 48, 51, and 56. However, these peaks had different retention times indicating that the peaks were different compounds. Several kinds of possibilities are listed in Table 3, but the structural identifications of these compounds require further investigations. Compared with the previous publications [4,8], this report detected more *aconitum* alkaloids and revealed the presence of many, so far unknown *aconitum* alkaloids that were overlooked by manual inspection.

4. Conclusion

This report took the advantages of the UPLC–ESI-Q-TOF-MS system with MS^E to obtain high resolution LC–MS data and fragment ions information, and established an improved post-acquired data processing method with Metabolynx XS with MDF to perform rapid and global detection of *aconitum* alkaloids in YCSNT. Compared with the conventional manual inspection, Metabolynx XS enables the acquired data to be analyzed in a much faster time frame and more chemical compounds to be mined to avoid the omission of some compounds at the lower concentration levels. In addition, Q-TOF-MS with MS^E can simultaneously generate the precursor ions and the corresponding fragment ions with accurate mass in a single injection, which is helpful in detecting and identifying of the compounds in the complex mixture of TCMF. Through its successful application to YCSNT, the reported method can be applied to other containing-Fuzi TCMFs. Through the proper modification of the parameter settings of Metabolynx XS and the chromatographic and spectrometric conditions, this method can also be used for the rapid analysis of other homologous families in TCMF.

Acknowledgments

The work was supported by the grant from National Program on Key Basic Research Project of China (Grant No. 2005CB523406) and Key Program of Natural Science Foundation of State (China) (Grant No. 90709019).

References

[1] A. Ameri, The effects of Aconitum alkaloids on the central nervous system, Prog. Neurobiol. 56 (1998) 211–235.
[2] H.K. Desai, B.P. Hart, R.W. Caldwell, J.Z. Huang, S.W. Pelletier, Certain norditerpenoid alkaloids and their cardiovascular action, J. Nat. Prod. 61 (1998) 743–748.
[3] N.G. Bisset, Arrow poisons in China. Part II. Aconitum—botany, chemistry, and pharmacology, J. Ethnopharmacol. 4 (1981) 247–336.
[4] R. Hu, J. Zhao, L.W. Qi, P. Li, S.L. Jing, H.J. Li, Structural characterization and identification of C(19)- and C(20)-diterpenoid alkaloids in roots of *Aconitum carmichaeli* by rapid-resolution liquid chromatography coupled with time-of-flight mass spectrometry, Rapid Commun. Mass Spectrom. 23 (2009) 1619–1635.
[5] Y. Xie, Z.H. Jiang, H. Zhou, H.X. Xu, L. Liu, Simultaneous determination of six Aconitum alkaloids in proprietary Chinese medicines by high-performance liquid chromatography, J. Chromatogr. A 1093 (2005) 195–203.
[6] K. Ito, Y. Ohyama, T. Hishinuma, M. Mizugaki, Determination of Aconitum alkaloids in the tubers of Aconitum japonicum using gas chromatography/selected ion monitoring, Planta Med. 62 (1996) 57–59.
[7] J.Z. Song, Q.B. Han, C.F. Qiao, P.P.H. But, H.X. Xu, Development and validation of a rapid capillary zone electrophoresis method for the determination of aconite alkaloids in aconite roots, Phytochem. Anal. 21 (2009) 137–143.
[8] X.T. Zheng, P.Y. Shi, Y.Y. Cheng, H.B. Qu, Rapid analysis of a Chinese herbal prescription by liquid chromatography–time-of-flight tandem mass spectrometry, J. Chromatogr. A 1206 (2008) 140–146.
[9] Z.J. Zhang, Shanghan Lun, People Hygiene Press, Beijing, 1987.
[10] Chinese Pharmacopoeia Commission, Chinese Pharmacopoeia, Chemical Industry Press, Beijing, 2005.
[11] H. Wang, F. Feng, Identification of components in Zhi-Zi-Da-Huang decoction by HPLC coupled with electrospray ionization tandem mass spectrometry, photodiode array and fluorescence detectors, J. Pharm. Biomed. Anal. 49 (2009) 1157–1165.
[12] X.J. Wang, W.J. Sun, H. Sun, H.T. Lv, Z.M. Wu, P. Wang, L. Liu, H.X. Cao, Analysis of the constituents in the rat plasma after oral administration of Yin Chen Hao Tang by UPLC/Q-TOF-MS/MS, J. Pharm. Biomed. Anal. 46 (2008) 477–490.
[13] R.J. Peters, M.C. van Engelen, M.E. Touber, C. Georgakopoulus, M.W. Nielen, Searching for in silico predicted metabolites and designer modifications of (cortico) steroids in urine by high-resolution liquid chromatography/time-of-flight mass spectrometry, Rapid Commun. Mass Spectrom. 23 (2009) 2329–2337.
[14] A.L. Freed, U. Kale, H. Ando, D.T. Rossi, C.A. Kingsmill, Improving the detection of degradants and impurities in pharmaceutical drug products by applying mass spectral and chromatographic searching, J. Pharm. Biomed. Anal. 35 (2004) 727–738.
[15] F. Hernández, S. Grimalt, O.J. Pozo, J.V. Sancho, Use of ultra-high-pressure liquid chromatography–quadrupole time-of-flight MS to discover the presence of pesticide metabolites in food samples, J. Sep. Sci. 32 (2009) 2245–2261.
[16] H.Y. Zhang, D.L. Zhang, K. Ray, M.S. Zhu, Mass defect filter technique and its applications to drug metabolite identification by high-resolution mass spectrometry, J. Mass Spectrom. 44 (2009) 999–1016.
[17] M.S. Zhu, L. Ma, D.L. Zhang, K. Ray, W.P. Zhao, W. Griffith Humphreys, G. Skiles, M. Sanders, H.Y. Zhang, Detection and characterization of metabolites in biological matrices using mass defect filtering of liquid chromatography/high resolution mass spectrometry data, Drug Metab. Dispos. 34 (2006) 1722–1733.
[18] H.Y. Zhang, M.S. Zhu, K.L. Ray, L. Ma, D.L. Zhang, Mass defect profiles of biological matrices and the general applicability of mass defect filtering for metabolite detection, Rapid Commun. Mass Spectrom. 22 (2008) 2082–2088.

[19] Q. Ruan, S. Peterman, M.A. Szewc, L. Ma, D. Cui, W. Griffith Humphreys, M.S. Zhu, An integrated method for metabolite detection and identification using a linear ion trap/Orbitrap mass spectrometer and multiple data processing techniques: application to indinavir metabolite detection, J. Mass Spectrom. 43 (2008) 251–261.
[20] Z.H. Han, Shanghan Weizhi Lun, Zhonghua Book Company, Beijing, 1985, pp. 58–62.
[21] X.J. Wang, Z.M. Wu, L. Zhao, G.L. Yan, Research of processing history of Yinchensini-Tang in the Yin jaundice therapy system, World Sci. Technol. -Mod. Tradit. Chin. Med. Mater. Med. 10 (2008) 12–14.
[22] X.J. Tan, Q. Li, X.H. Chen, Z.W. Wang, Z.Y. Shi, K.S. Bi, Y. Jia, Simultaneous determination of 13 bioactive compounds in Herba Artemisiae Scopariae (Yin Chen) from different harvest seasons by HPLC-DAD, J. Pharm. Biomed. Anal. 47 (2008) 847–853.
[23] Q. Zhang, M. Ye, Chemical analysis of the Chinese herbal medicine Gan-Cao (licorice), J. Chromatogr. A 1216 (2009) 1954–1969.
[24] S.D. Jolad, R.C. Lantz, G.J. Chen, R.B. Bates, B.N. Timmermann, Commercially processed dry ginger (Zingiber officinale): composition and effects on LPS-stimulated PGE2 production, Phytochemistry 66 (2005) 1614–1635.
[25] L.H. Chen, L.J. Jin, Z.M. Su, Y.Q. Qiu, Y.L. Wang, S.Y. Liu, ESI·MS behavior quantum chemistry calculation of stability of fragment ions of diester diterpenoid alkaloids (DDA), Chem. J. Chin. Univ. 26 (2005) 2340–2344.
[26] R.S. Plumb, K.A. Johnson, P. Rainville, B.W. Smith, I.D. Wilson, J.M. Castro-Perez, J.K. Nicholson, UPLC/MS^E: a new approach for generating molecular fragment information for biomarker structure elucidation, Rapid Commun. Mass Spectrom. 20 (2006) 1989–1994.